then the energy of the charge-transfer process should depend linearly on the redox potential of the complex. Such linear relationships have been reported for ligand-to-metal charge-transfer (LTMCT) transitions in both technetium[4] and ruthenium[16] complexes, as well as in a series of tris(bipyridyl) complexes of several metals.[17,18] Figure 8 shows that a linear relationship (correlation coefficient 0.997, slope −0.83) also holds for the MTLCT transition of the Tc(III) complexes (except for the anomalous $(buac)_2en$ material). The MTLCT process in these complexes involves formal oxidation of Tc(III) to Tc(IV), and indeed the redox potential of the Tc(IV)/Tc(III) couple is linearly related to the energy of this process.

Acknowledgment. Financial support by the National Institutes of Health, Grant No. HL-21276 (E.D.), and the Department of Energy, Grant No. DE-AC02-80EV10380 (W.R.H.), is gratefully acknowledged. We also thank Dr. S. Jurisson for providing the technetium complexes used in this study.

Registry No. **1**, 96429-92-4; 1^+, 93426-97-2; 1^{2+}, 96429-97-9; **2**, 96429-93-5; 2^+, 93426-99-4; 2^{2+}, 96429-98-0; **3**, 96429-94-6; 3^+, 93427-01-1; 3^{2+}, 96429-99-1; **4**, 96429-95-7; 4^+, 93427-03-3; 4^{2+}, 96430-00-1; **5**, 96429-96-8; 5^+, 93427-05-5; 5^{2+}, 96430-01-2; **6**, 93453-71-5; 6^+, 93453-71-5; 6^{2+}, 96430-02-3; **7**, 96444-60-9; 7^+, 93427-07-7; 7^{2+}, 96430-03-4; **8**, 96444-61-0; 8^+, 93427-09-9; 8^{2+}, 96444-62-1; Au, 7440-57-5; TEAP, 2567-83-1; Pt, 7440-06-4.

(16) Matsubara, T.; Ford, P. C. *Inorg. Chem.* **1976**, *15*, 1107.
(17) Saji, T.; Aoyagi, J. *J. Electroanal. Chem. Interfacial Electrochem.* **1975**, *60*, 1.
(18) Matsumura-Inoue, T.; Tomono, H.; Kasai, M.; Tominaga-Morimoto, T. *J. Electroanal. Chem. Interfacial Electrochem.* **1979**, *95*, 109.

Contribution from the Department of Chemistry, University of Houston—University Park, Houston, Texas 77004, and Laboratoire de Synthèse et d'Electrosynthèse, Organométallique Associé au CNRS (LA 33), Faculté des Sciences "Gabriel", University of Dijon, 21100 Dijon, France

Electrochemistry and Spectroelectrochemistry of Indium(III) Porphyrins. Reactions of Five-Coordinate σ-Bonded Complexes

K. M. KADISH,*[1a] B. BOISSELIER-COCOLIOS,[1a] P. COCOLIOS,[1b,c] and R. GUILARD*[1b]

Received December 11, 1984

The electrochemistry, NMR spectroscopy, and UV–visible spectroscopy of 16 different In(III) porphyrins with σ-bound alkyl or aryl groups were investigated in nonaqueous media. The ligands σ bonded to indium(III) octaethylporphyrins or tetraphenylporphyrins included simple alkyl groups such as CH_3 or C_2H_5 and aryl groups such as C_6H_5, $C_2H_2C_6H_5$, or $C_2C_6H_5$. All of the compounds could be oxidized or reduced by multiple single-electron-transfer steps in which the initial step yields $[(P)In(R)]^+$ or $[(P)In(R)]^-$, where P represents the porphyrin macrocycle and R is one of the σ-bonded ligands. In all cases, the singly reduced compound is stable. In contrast, the singly oxidized compounds undergo a metal–carbon bond cleavage, the rate of which depended upon the electron-donating properties of the axial ligand. The electron-donating properties of the σ-bonded ligand also influence the electronic absorption spectra and the ^1H NMR spectra of the neutral compounds, and linear free energy relationships with ^1H NMR shifts or ratios of molar absorptivities in the UV–visible spectra were obtained. Not surprisingly, complexes containing the $C_2C_6H_5$ group did not fit these trends, and the physical properties of these complexes more closely resembled those of the indium(III) porphyrins axially bound by ionic ligands such as Cl^-, ClO_4^-, or PF_6^-. Finally, comparisons between the electrochemical reactivities of the σ-bonded complexes and their physicochemical properties are discussed in terms of the general stability of the indium–carbon σ bond.

Introduction

Metal–alkyl (or –aryl) σ-bonded porphyrins are of considerable interest as model compounds for understanding the function and reactivity of several biological macromolecules. From this point of view, the syntheses of numerous iron,[2–11] cobalt,[2,12–17] and rhodium[18–26] porphyrins as well as other metalloporphyrins containing a metal–carbon σ bond have been described.[27–31]

(1) (a) University of Houston. (b) University of Dijon. (c) Present address: L'Air Liquide, CRCD, F-78350 Jouy-en-Josas, France.
(2) Clarke, D. A.; Dolphin, D.; Grigg, R.; Johnson, A. W.; Pinnock, H. A. *J. Chem. Soc. C* **1968**, 881.
(3) Reed, C. A.; Mashiko, T.; Bentley, S. P.; Kastner, M. E.; Scheidt, W. R.; Spartalian, K.; Lang, G. *J. Am. Chem. Soc.* **1979**, *101*, 2948.
(4) Ortiz de Montellano, P. R.; Kunze, K. L.; Augusto, O. *J. Am. Chem. Soc.* **1982**, *104*, 3545.
(5) Lexa, D.; Saveant, J. M. *J. Am. Chem. Soc.* **1981**, *103*, 6806.
(6) Lexa, D.; Saveant, J. M. *J. Am. Chem. Soc.* **1982**, *104*, 3503.
(7) Lexa, D.; Saveant, J. M.; Battioni, J. P.; Lange, M.; Mansuy, D. *Angew. Chem., Int. Ed. Engl.* **1980**, *20*, 578.
(8) Cocolios, P.; Laviron, E.; Guilard, R. *J. Organomet. Chem.* **1982**, *228*, C39.
(9) Ogoshi, H.; Sugimoto, H.; Yoshida, Z.-I.; Kobayashi, H.; Sakai, H.; Maeda, Y. *J. Organomet. Chem.* **1982**, *234*, 185.
(10) Mansuy, D.; Battioni, J. P. *J. Chem. Soc., Chem. Commun.* **1982**, *638*.
(11) Cocolios, P.; Lagrange, G.; Guilard, R. *J. Organomet. Chem.* **1983**, *265*, 65.
(12) Ogoshi, H.; Watanabe, E.; Setsune, T.; Koketsu, N.; Yoshida, Z. *J. Chem. Soc., Chem. Commun.* **1974**, *943*.
(13) Perree-Fauvet, M.; Gaudemer, A.; Boucly, P.; Devynck, J. *J. Organomet. Chem.* **1976**, *120*, 439.
(14) Callot, H. J.; Schaeffer, E. *J. Organomet. Chem.* **1978**, *145*, 91.
(15) Callot, H. J.; Schaeffer, E. *J. Organomet. Chem.* **1980**, *193*, 111.
(16) Dolphin, D.; Halko, J.; Johnson, E. *Inorg. Chem.* **1981**, *20*, 4348.
(17) Callot, H. J.: Metz, F. *J. Chem. Soc., Chem. Commun.* **1982**, *947*.
(18) Ogoshi, H.; Setsune, J.; Omura, T.; Yoshida, Z. *J. Am. Chem. Soc.* **1975**, *97*, 6461.
(19) Grigg, R.; Trocha-Grimshaw, J.; Viswanatha, V. *Tetrahedron Lett.* **1976**, *4*, 289.
(20) Abeysekera, A. M.; Grigg, R.; Trocha-Grimshaw, J.; Viswanatha, V. *J. Chem. Soc., Perkin Trans. 1* **1977**, 1395.
(21) Callot, H. J.; Schaeffer, E. *J. Chem. Soc., Chem. Commun.* **1978**, 937.
(22) Ogoshi, H.; Setsune, J.-I.; Nanbo, Y.; Yoshida, Z.-I. *J. Organomet. Chem.* **1978**, *159*, 329.
(23) Callot, H. J.; Schaeffer, E. *Nouv. J. Chim.* **1980**, *4*, 311.
(24) Ogoshi, H.; Setsune, J.-I.; Yoshida, Z.-I. *J. Organomet. Chem.* **1980**, *185*, 95.
(25) Wayland, B. B.; Woods, B. A. *J. Chem. Soc., Chem. Commun.* **1981**, 700.
(26) Setsune, J.; Yoshida, Z.-I.; Ogoshi, H. *J. Chem. Soc., Perkin Trans 1* **1982**, 983.
(27) Ogoshi, H.; Setsune, J.; Yoshida, Z.-I. *J. Organomet. Chem.* **1978**, *159*, 317.
(28) Cloutour, C.; Lafargue, D.; Richards, J. A.; Pommier, J. C. *J. Organomet. Chem.* **1977**, *137*, 157.
(29) Inoue, S.; Takeda, N. *Bull. Chem. Soc. Jpn.* **1977**, *50*, 984.
(30) Takeda, N.; Inoue, S. *Bull. Chem. Soc. Jpn* **1978**, *51*, 3564.
(31) Inoue, S.; Murayama, N.; Takeda, N.; Ohkatsu, Y. *Chem. Lett.* **1982**, 317.

0020-1669/85/1324-2139$01.50/0

Several years ago one of our laboratories reported the synthesis and characterization of indium(III) porphyrins that were σ bonded with alkyl or aryl groups.[32] More recently, the chemical reactivity of these compounds toward sulfur dioxide[33] and carbon dioxide[34] has also been described. From this latter study it was shown that carbon dioxide insertion into the indium–carbon σ bond is photoactivated by visible light, and it was suggested that the reaction proceeded via a low oxidation state intermediate. In order to gain insight as to the nature and stability of the low oxidation state intermediate in this reaction, we have now undertaken electrochemical studies on a series of In(III) porphyrins containing σ-bonded axial ligands.

In a parallel study we have characterized the electrode reaction of both tetraphenyl and octaethyl indium(III) porphyrins containing the counterions Cl^-, ClO_4^-, and PF_6^-.[35] These studies were carried out in both binding and nonbinding nonaqueous media, and the products of the electrode reactions were characterized by electronic absorption spectra and ESR. In this present study the electrooxidations and electroreductions of seven σ-bonded (TPP)In(R) and seven (OEP)In(R) complexes were investigated in CH_2Cl_2 and pyridine containing 0.1 M $(TBA)PF_6$. In these complexes, the R groups were varied from the weakly electron-donating $C(CH_3)_3$ group to the strongly electron-withdrawing C_6H_5 group.

An eighth σ-bonded complex, $(P)In(C_2C_6H_5)$, decomposes in CH_2Cl_2, and consequently all electrochemical studies were limited to PhCN containing 0.1 M $(TBA)PF_6$. Characterization of each species by electronic absorption spectra, ESR, and NMR spectroscopy is also reported, and comparisons are made between the resulting physicochemical measurements by each technique. Finally, the stability of each σ-bonded compound was evaluated and the rate of metal–alkyl group cleavage determined by electrochemical techniques.

Experimental Section

Electrochemical Instrumentation. Cyclic voltammetric measurements were obtained with the use of a three-electrode system where the working electrode was a platinum button and the counterelectrode a platinum wire. A saturated calomel electrode (SCE) served as a reference electrode and was separated from the bulk of the solution by a fritted glass bridge. An EG&G Model 173 potentiostat, an EG&G Model 175 universal programmer, and a Houston Instruments Model 2000 X-Y recorder or a BAS-100 electrochemical analyzer, a Houston Instruments HIPLOT DMP-40 plotter, and an EPSON Model FX80 printer were used.

Controlled-potential electrolysis was performed by using an EG&G Model 173 potentiostat or a BAS-100 electrochemical analyzer. Both the reference electrode and the platinum-wire counterelectrode were separated from the bulk solution by means of fritted glass bridges.

Thin-layer spectroelectrochemical measurements were performed with an IBM EC 225 voltammetric analyzer coupled with a Tracor Northern 1710 holographic optical spectrometer/multichannel analyzer to obtain time-resolved spectral data. The optically transparent platinum thin-layer electrode (OTTLE) that was utilized has been described in a previous publication.[36]

Spectroscopic Instrumentation. UV–visible spectra were taken by a Tracor Northern 1710 spectrophotometer. ESR spectra were recorded on an IBM Model ER 100D spectrometer equipped with an ER 040-X microwave bridge and an ER 080 power supply. IR spectra were obtained with use of a Perkin-Elmer 1330 spectrometer. Samples were a 1% dispersion in CsI pellets. ^1H NMR spectra were recorded on a JEOL FX 100 spectrometer. Spectra were measured for solutions in 0.5 mL of $CDCl_3$ or C_6D_6 with tetramethylsilane as internal reference.

Chemicals. Reagent grade methylene chloride (CH_2Cl_2) and benzonitrile (PhCN) were distilled over P_2O_5 before use. Tetrabutylammonium perchlorate (TBAP) (Fluka) was recrystallized from ethanol. Tetrabutylammonium hexafluorophosphate ($(TBA)PF_6$) (Fluka) was recrystallized from ethyl acetate. (TPP)InCl and (OEP)InCl were synthesized according to literature procedures.[37] (TPP)In(R) and (OEP)In(R) where R stands for CH_3, C_2H_5, C_4H_9, $CH(CH_3)_2$, $C(CH_3)_3$, C_6H_5, $C_2H_2C_6H_5$, and $C_2C_6H_5$ were synthesized according to previously reported methods[32] and characterized by IR and UV–visible spectroscopic methods.

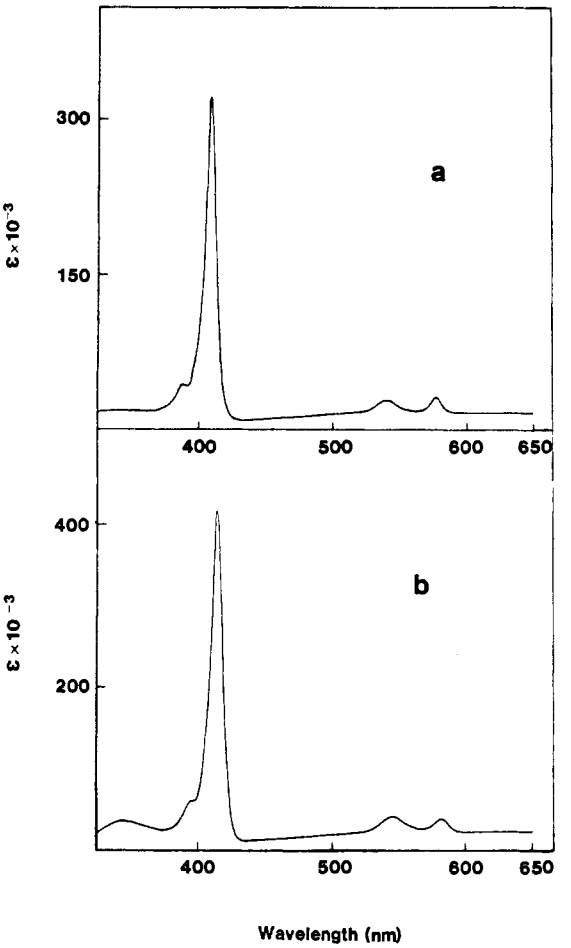

Figure 1. Electronic absorption spectra of (a) (OEP)InCl and (b) $(OEP)In(C_2C_6H_5)$ in C_6H_6.

Results and Discussion

Spectroscopic Properties of Neutral (TPP)In(R) and (OEP)In(R). The electronic absorption spectra of (TPP)InX and (OEP)InX where X is an anionic ligand are classified as "normal" porphyrin spectra. (TPP)InCl has a Soret band at 425 nm in C_6H_6 and three Q bands at 516, 560, and 600 nm. In the same solvent, (OEP)InCl has a Soret band at 409 nm and three Q bands at 497, 530, and 577 nm. This is illustrated in Figure 1a.

In contrast to indium porphyrins with anionic ligands such as Cl^- or ClO_4^-, the σ-bonded indium(III) porphyrins have electronic absorption spectra belonging to the hyperclass.[38] Thus, replacement of the anionic axial ligand on (P)InX by an alkyl or aryl σ-bonded ligand leads to a splitting of the Soret band into two bands, one of which is red shifted and the other of which is blue shifted with respect to the complex with anionic axial ligands. This is illustrated in Figure 2 for the cases of $(OEP)In(C_2H_5)$ and $(OEP)In(C(CH_3)_3)$ in C_6H_6. As seen in this figure, the former compound has a split Soret band with peak maxima at 365 and 435 nm, while the latter compound has Soret peaks at 377 and 443 nm. In addition, the ratio of the molar absorptivities for the split Soret peaks varies as a function of the different R groups. For $(OEP)In(C_2H_5)$, the ratio of the band molar absorptivities for band II and band I ($\epsilon(II)/\epsilon(I)$) is 2.48 while for

(32) Cocolios, P.; Guilard, R.; Fournari, P. *J. Organomet. Chem.* **1979**, *179*, 311.
(33) Cocolios, P.; Fournari, P.; Guilard, R.; Lecomte, C.; Protas, J.; Boubel, J. C. *J. Chem. Soc., Dalton Trans.* **1980**, 2081.
(34) Cocolios, P.; Guilard, R.; Bayeul, D.; Lecomte, C. *Inorg. Chem.* **1985**, *24*, 2058.
(35) Kadish, K. M.; Cornillon, J.-L.; Cocolios, P.; Tabard, A.; Guilard, R. *Inorg. Chem.*, in press.
(36) Lin, X.; Kadish, K. M. *Anal. Chem.* **1985**, *57*, 1498.
(37) Buchler, J. W.; Eikelmann, G.; Puppe, L.; Rohbock, K.; Schneehage, H. H.; Weck, D. *Justus. Liebigs Ann. Chem.* **1971**, *745*, 135.
(38) Gouterman, M. In "The Porphyrins"; Dolphin, D., Ed.; Academic Press: New York, 1978; Vol. III, Chapter I and references therein.

Table I. Maximum Absorbance Wavelengths (λ_{max}, nm) and Corresponding Molar Absorptivities ($\epsilon \times 10^{-3}$) for Neutral (TPP)In(R) Complexes in $CHCl_3$ or C_6H_6

R	solvent[a]	band I	band II	ϵ(II)/ϵ(I)	Q(2,0)	Q(1,0)	Q(0,0)
$C(CH_3)_3$	A	393 (100)	453 (136)	1.36	551 (3.8)	592 (9.8)	639 (13.6)
$CH(CH_3)_2$	A	383 (66.7)	451 (203)	3.04	550 (3.7)	590 (11.7)	636 (15.1)
C_4H_9	A	356 (42.4)	445 (335)	7.90	544 (3.6)	583 (13.5)	627 (15.2)
C_2H_5	A	355 (36.5)	445 (293)	8.03	545 (3.2)	584 (11.7)	628 (13.8)
CH_3	A	343 (34.2)	439 (470)	13.74	538 (4.0)	578 (15.5)	623 (14.6)
C_6H_5	B	343 (36.2)	439 (531)	14.67	535 (3.4)	577 (16.8)	619 (14.9)
$C_2H_2C_6H_5$	A	340 (32.2)	439 (496)	15.40	538 (3.5)	578 (16.3)	621 (13.8)
$C_2C_6H_5$	B	322 (23.1)	432 (323)	13.98	528 (3.7)	568 (21.1)	610 (12.0)

[a] A = $CHCl_3$, B = C_6H_6.

Table II. Maximum Absorbance Wavelengths (λ_{max}, nm) and Corresponding Molar Absorptivities ($\epsilon \times 10^{-3}$) for Neutral (OEP)In(R) Complexes in $CHCl_3$ or C_6H_6

R	solvent[a]	band I	band II	ϵ(II)/ϵ(I)	Q(2,0)	Q(1,0)	Q(0,0)
$C(CH_3)_3$	B	377 (95.3)	443 (61.4)	0.64		565 (13.6)	594 (3.6)
$CH(CH_3)_2$	A	372 (88.8)	439 (96.8)	1.09	525 (3.4)	564 (17.8)	595 (5.3)
C_4H_9	B	365 (59.3)	435 (142)	2.39	520 (2.4)	559 (17.6)	594 (6.5)
C_2H_5	B	365 (58.5)	435 (145)	2.48	520 (2.4)	558 (17.7)	592 (6.4)
CH_3	B	354 (49.0)	428 (247)	5.04	515 (2.5)	554 (17.2)	588 (8.9)
C_6H_5	B	354 (45.1)	424 (264)	5.85	512 (2.8)	551 (18.3)	587 (9.6)
$C_2H_2C_6H_5$	B	354 (39.8)	426 (246)	6.18	514 (2.0)	554 (17.6)	589 (9.8)
$C_2C_6H_5$	B	345 (30.7)	415 (426)	13.88	508 (2.5)	547 (20.0)	584 (18.0)

[a] A = $CHCl_3$, B = C_6H_6.

(OEP)In($C(CH_3)_3$) this ratio is 0.64.

The In(III) metal ions of (OEP)In(R) and (TPP)In(R) have filled d orbitals, and consequently the blue-shifted band I (Figure 2) may be attributed to a $5p_z \rightarrow e_g(\pi^*)$ transition. On the other hand, the red-shifted band II (Figure 2) may be attributed to a $\pi \rightarrow \pi^*$ electronic transition of the porphyrin ring. The ϵ(II)/ϵ(I) molar absorptivity ratio of these two bands should be systematically related to the electron-donating character of the bound R group; the more electron-donating the R group, the higher the $5p_z \rightarrow e_g(\pi^*)$ transition (band I) and the smaller the ϵ(II)/ϵ(I) should be. This is generally true for all of the (OEP)In(R) and (TPP)In(R) complexes investigated in this study and is evident from Tables I and II which list the electronic absorption spectra of each investigated (TPP)In(R) and (OEP)In(R) complex in either $CHCl_3$ or C_6H_6. As seen in Table I, a progressive shift of ϵ(II)/ϵ(I) occurs on going from (TPP)In($C(CH_3)_3$) (molar absorptivity ratio 1.36) to (TPP)In($C_2H_2C_6H_5$) (molar absorptivity ratio 15.40). The last complex in the series, (TPP)In($C_2C_6H_5$), shows some deviation from the spectral trend of the other (TPP)In(R) complexes. In fact, the visible spectrum of the complex more closely resembles that of ionic (TPP)InX than that for any of the other σ-bonded (TPP)In(R) complexes.

Trends in the molar absorptivities of the absorption bands as a function of the R donor ligand are also observed for the series of (OEP)In(R) complexes. This is evident from Table II which summarizes the spectral wavelengths and molar absorptivities of each investigated (OEP)In(R) complex. Similar to the (TPP)-In(R) series, each species has a split Soret band and an ϵ(II)/ϵ(I) molar absorptivity ratio that varies in a linear manner with the electron-donating property of the bound R group. In this case, the ratio of the molar absorptivities between bands II and I ranges from 0.64 for (OEP)In($C(CH_3)_3$) to 6.18 for (OEP)In-($C_2H_2C_6H_5$). For a given R group, the ratio is about half that of the corresponding (TPP)In(R) complex, which is due to differences in electron donicity of the two porphyrin rings. One would expect the hypercharacter of the spectra to be logically more pronounced for the OEP complexes than for the TPP complexes, and this appears to be the case. Finally, the molar absorptivity ratio of the two bands for (OEP)In($C_2C_6H_5$) is 13.88, which is virtually identical with that of (TPP)In($C_2C_6H_5$) (13.98). Again, the spectral properties of this complex are quite different from those for the other (OEP)In(R) complexes, and the spectrum more closely resembles that of ionic (OEP)InX. This is shown in Figure 1b.

The above results suggest that the greater the electron-donating properties of the bound R group, the larger the electron density

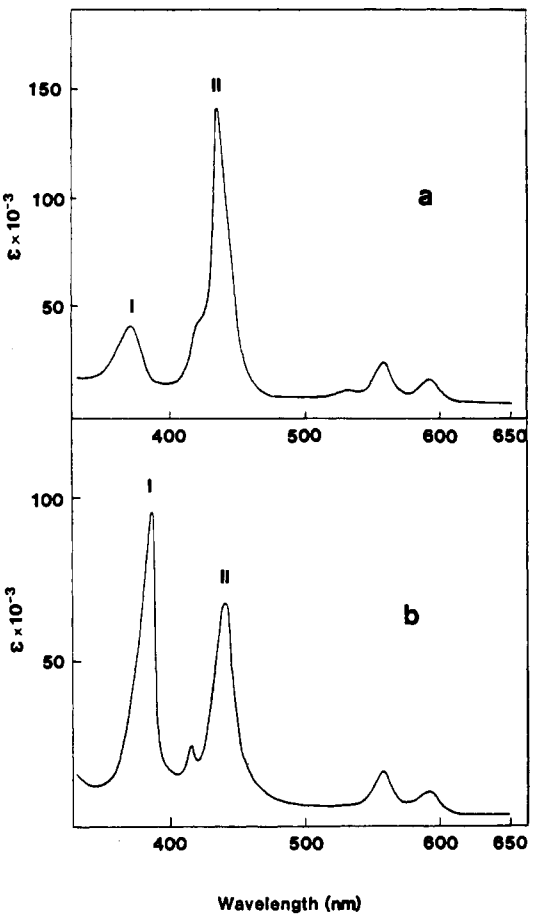

Figure 2. Electronic absorption spectra of (a) (OEP)In(CH_3) and (b) (OEP)In($C(CH_3)_3$) in C_6H_6.

will be on the In(III) metal and on the conjugated porphyrin π system. This is also suggested by NMR studies on the same series of complexes. It is well-known that the resonance signals for the meso protons of the octaethylporphyrin complexes depend upon the oxidation state of the central metal.[39] Divalent metals have

(39) Scheer, H.; Katz, J. J. In "Porphyrins and Metalloporphyrins"; Smith, K. M., Ed.; Elsevier: Amsterdam, 1975; Chapter 10.

Table III. Potentials (V vs. SCE) for Oxidation and Reduction of σ-Bonded (TPP)In(R) Complexes in CH_2Cl_2 (0.1 M $(TBA)PF_6$)[a] (Scan Rate 100 mV/s)

		oxidation			reduction	
R	σ^{*b}	1st	2nd	3rd	1st	2nd
$C(CH_3)_3$	−0.30	0.64[c]	1.20	1.52	−1.27	−1.71
$CH(CH_3)_2$	−0.19	0.74[c]	1.18	1.50	−1.26	−1.67
C_4H_9	−0.13	0.78[c]	1.20	1.53	−1.26	−1.69
C_2H_5	−0.10	0.83[c]	1.20	1.51	−1.25	−1.66
CH_3	0.00	0.88[c]	1.19	1.52	−1.24	−1.64
$C_2H_2C_6H_5$	...	0.92[c]	1.19	1.53	−1.24	−1.64
C_6H_5	+0.60	0.94[d]	1.44[d]	...	−1.22	−1.62

[a] Unless indicated, all values are reversible $E_{1/2}$ values. [b] Substituent constant for R group.[41] [c] E_{pa} measured at 100 mV/s. A 0.03 V positive shift in E_p was observed for each 10-fold increase in scan rate. [d] $E_{1/2}$ measured at −10 °C.

resonances in the region of 9.75–10.08 ppm while for tri- and tetravalent metals this resonance is in the range of 10.13–10.39 and 10.30–10.58 ppm, respectively.[39] The Re(V) species, (OEP)Re(O)(OPh), has a resonance of 10.55 ppm and the Os(VI) species, $(OEP)Os(O)_2$, has a resonance of 10.75 ppm. These positive shifts with increase in metal oxidation state are not unexpected since the more positive metal ions decrease the electron density of the macrocycle, logically inducing a deshielding of the methinic protons.

For the case of (OEP)In(R), the indium oxidation state is III and the observed methine proton shifts of 10.17–10.41 ppm correspond to those of a typical trivalent metal.[32] Only small variations exist between the series of (OEP)In(R) compounds, but the trend is clear-cut. For all of the (OEP)In(R) complexes, with the exception of $(OEP)In(C_2C_6H_5)$, the resonances range between 10.17 and 10.22 ppm. In contrast, the non-σ-bonded (OEP)InCl complex has a much larger resonance of 10.34 ppm, while for $(OEP)InClO_4$ this resonance has shifted to 10.41 ppm. Again, $(OEP)In(C_2C_6H_5)$ is quite different from the other σ-bonded complexes, and the resonance for this compound is found at 10.37 ppm, a value located just between that of (OEP)InCl and $(OEP)InClO_4$.

The exact resonance position of the (OEP)In(R) methinic protons varies systematically with the electron donicity of the axial ligands; i.e., the more basic the axial ligand, the higher the field. This results in the following sequence of the complexes based on the increasing resonance signal of the methinic protons (δ): $(OEP)In(C(CH_3)_3)$ (10.17) = $(OEP)In(C_4H_9)$ (10.17) < $(OEP)In(CH(CH_3)_2)$ (10.18) = $(OEP)In(C_2H_5)$ (10.18) < $(OEP)In(CH_3)$ (10.19) < $(OEP)In(C_6H_5)$ (10.21) < $(OEP)In(C_2H_2C_6H_5)$ (10.22) < (OEP)InCl (10.34) < $(OEP)In(C_2C_6H_5)$ (10.37) < $(OEP)InClO_4$ (10.41).

The above sequence of resonances parallels the results obtained from the electronic absorption spectra and further demonstrates that the $(OEP)In(C_2C_6H_5)$ and $(TPP)In(C_2C_6H_5)$ species are quite different from the other porphyrins in the (P)In(R) series and spectrally more closely resemble (P)InCl and $(P)InClO_4$. In addition, results from both the NMR spectra and electronic absorption spectra indicate that the electron density on the porphyrin ring (and on the indium metal atom) is directly related to the donor properties of the σ-bound R group.

Reductions of (OEP)In(R) and (TPP)In(R) in CH_2Cl_2 (0.1 M $(TBA)PF_6$). Similar reductive electrochemical behavior was observed for each of the (P)In(R) complexes in CH_2Cl_2. For reduction, either one or two single-electron additions were observed (depending on the porphyrin macrocycle) without cleavage of the indium–carbon bond on the cyclic voltammetric time scale. The (TPP)In(R) series exhibited two one-electron additions represented by eq 1 and 2.

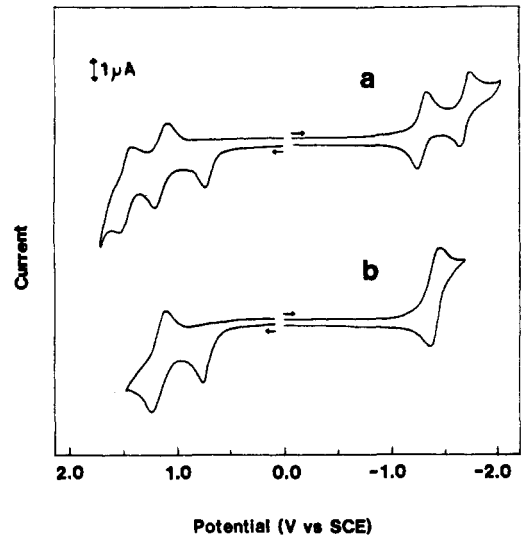

Figure 3. Cyclic voltammograms of (a) $(TPP)In(CH_3)$ and (b) $(OEP)In(CH_3)$ in CH_2Cl_2 (0.1 M $(TBA)PF_6$) [scan rate 100 mV/s].

$$(TPP)In(R) + e^- \rightleftarrows [(TPP)In(R)]^-\cdot \quad (1)$$

$$[(TPP)In(R)]^-\cdot + e^- \rightleftarrows [(TPP)In(R)]^{2-} \quad (2)$$

The voltammogram of $(TPP)In(CH_3)$ is depicted in Figure 3a and is quite representative of the whole (TPP)In(R) series in reduction. Potentials for the above reductions are given in Table III. As seen in this table, the values of $E_{1/2}$ are shifted negatively by greater than 0.12 V from the respective first and second reduction waves of $(TPP)InClO_4$ (which occur at −1.10 and −1.46 V in CH_2Cl_2 (0.1 M $(TBA)PF_6$). This is not unexpected and is due to the increased negative charge on the singly and doubly reduced (P)In(R) complex with respect to the singly and doubly reduced (P)InX. This latter series of compounds loses X^- upon addition of the first electron so that the product of the first reduction is the neutral (P)In radical.[35] However, it is interesting to note that the 0.17 V difference in $E_{1/2}$ for reduction of $(TPP)InClO_4$ and the most difficult to reduce σ-bonded indium(III) complex, $(TPP)In(C(CH_3)_3)$, is much less than the difference in reduction potentials between $(TPP)FeClO_4$ and (TPP)Fe(R) complexes where negative shifts as large as 1.0 V have been obtained.[45] For reductions at the π-ring system of the porphyrin a smaller interaction with the axial ligand is expected, and this seems to be the case in the present study. In the iron case, however, reduction clearly involves the orbitals of the central metal so that both the charge of the complex and the nature of the R group more directly effect the value of the measured half-wave potentials.

The potentials for reduction of (TPP)In(R) parallel the magnitude of the substituent constant, σ^*, associated with the bound R group.[41] This is shown in Table III. Values of σ vary between −0.30 for R = $C(CH_3)_3$ and +0.60 for R = C_6H_5. For the same series of complexes, values of $E_{1/2}$ vary between −1.22 and −1.27 V for the first reduction and between −1.62 and −1.71 V for the second reduction. The difference in $E_{1/2}$ between the first and second reduction ranges between 0.40 and 0.42 V for the (TPP)In(R) series and is comparable to the 0.38 V difference in the two reduction potentials of $(TPP)InClO_4$ in PhCN.[35]

In contrast to the (TPP)In(R) series, only one well-defined reduction is observed for the six (OEP)In(R) complexes. A cyclic voltammogram is depicted in Figure 3b for the $(OEP)In(CH_3)$

(40) Kadish, K. M. *J. Electroanal. Chem. Interfacial Electrochem.* **1984**, *168*, 261.
(41) Values of σ^* were taken from: Taft, R. W., Jr. In "Steric Effects in Organic Chemistry"; Newman, M. S., Ed.; Wiley: New York, 1956; Chapter 13.
(42) Zuman, P. In "Substituent Effects in Organic Polarography"; Plenum Press: New York, 1967.
(43) Davis, D. G. In "The Porphyrins"; Dolphin, D., Ed.; Academic Press: New York, 1978; Vol. V, Chapter 4 and references therein.
(44) Fuhrhop, J.-H. In "Porphyrins and Metalloporphyrins"; Smith, K. M., Ed.; Elsevier: Amsterdam, 1975; Chapter 14.
(45) Lançon, D.; Cocolios, P.; Guilard, R.; Kadish, K. M. *J. Am. Chem. Soc.* **1984**, *106*, 4472.

Table IV. Potentials (V vs. SCE) for Oxidation and Reduction of σ-Bonded (OEP)In(R) Complexes in CH_2Cl_2 (0.1 M $(TBA)PF_6$)[a] (Scan Rate 100 mV/s)

R	σ^{*b}	oxidation		reduction	
		1st	2nd	1st	2nd
$C(CH_3)_3$	-0.30	0.53	1.14	-1.54	...
$CH(CH_3)_2$	-0.19	0.62[c]	1.13	-1.53	...
C_4H_9	-0.13	0.67[c]	1.16	-1.50	...
C_2H_5	-0.10	0.67[c]	1.16	-1.48	...
CH_3	0.00	0.70[c]	1.11	-1.50	...
C_6H_5	0.60	0.79[d]	1.15	-1.47	...
$C_2H_2C_6H_5$	...	0.81[c]	1.11	-1.48	...

[a] Unless indicated, all values are reversible $E_{1/2}$ values. [b] Substitutent constant for R group.[41] [c] E_{pa} measured at 100 mV/s. A 0.03 V positive shift in E_p was observed for each 10-fold increase in scan rate. [d] $E_{1/2}$ measured at -10 °C.

case, and reduction potentials for all of the (OEP)In(R) series are summarized in Table IV. This single reduction is diffusion controlled for all of the complexes of the series and is represented by eq 3. A second reduction of (OEP)In(R) would be expected

$$(OEP)In(R) + e^- \rightleftarrows [(OEP)In(R)]^- \cdot \qquad (3)$$

to occur at ~-1.90 V, and this is partially observed for some of the complexes. However, the potentials for this reduction are just at the cathodic limit of the solvent that was utilized, and because of this, the second redution of (OEP)In(R) was not investigated in this study. The first reduction potential of (OEP)In(R) ranges between -1.47 V for the most easily reduced (OEP)In(C_6H_5) complex and -1.54 V for the most difficult to reduce (OEP)In($C(CH_3)_3$) species. This 0.07 V difference in the values of $E_{1/2}$ parallels the magnitude of the substituent constant for the bound R group,[41] but the actual substituent effect (defined by the slope of $\Delta E_{1/2}/\Delta\sigma^*$[42]) is very small, indicating little interaction of the substituent with the reaction site of electroreduction. As stated above, a similar shift of $E_{1/2}$ with σ^* is observed for the (TPP)In(R) series, and with the exception of the C_6H_5 derivative, a linear plot of $E_{1/2}$ vs. σ^* is obtained. However, the slope of this plot is very small, again indicating only slight interaction of the substituent with the electroreduction site.

A large number of potentials have been measured for the reduction of different OEP and TPP metalloporphyrins.[43,44] In all cases, the OEP derivatives are the most difficult to reduce. This is consistent with the increased basicity of the OEP ring with respect to the TPP analogue. The absolute difference in potential between the two series is not constant for a given metal and generally varies between 0.10 and 0.25 V depending upon the nature of the counterion and/or other bound axial ligands. In this study the negative shift of the first reduction potential was 0.23-0.25 V on going from the (TPP)In(R) series to the (OEP)In(R) series and agrees with a similar difference of 0.23 V between $E_{1/2}$ values for reduction of (TPP)Fe(C_6H_5) and (OEP)Fe(C_6H_5) in PhCN.[45]

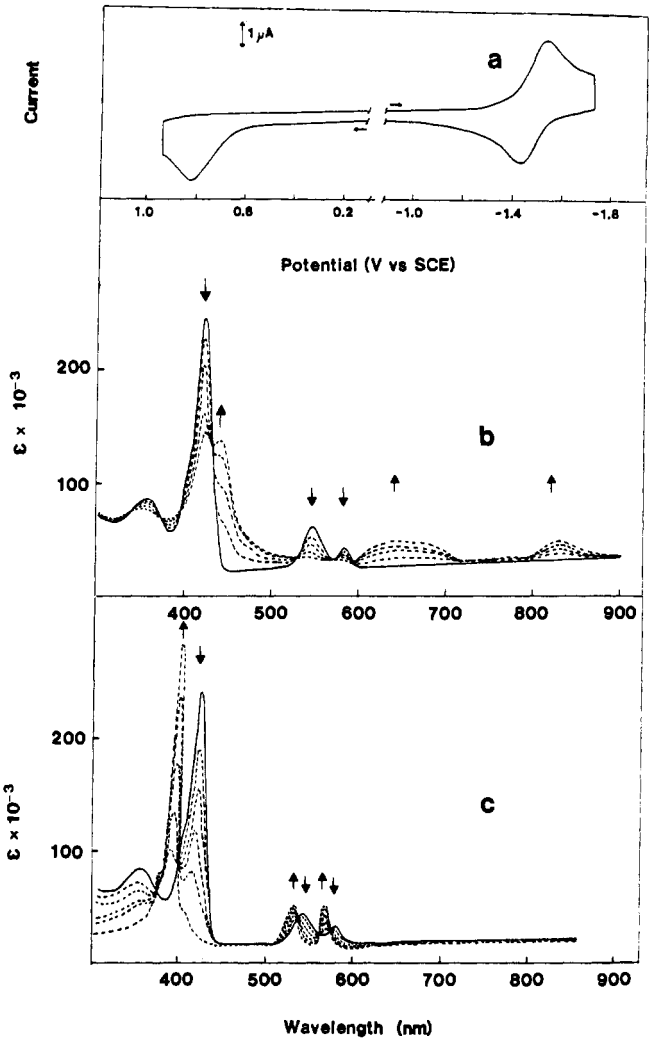

Figure 4. (a) Thin-layer cyclic voltammograms of (TPP)In(CH_3) in PhCN in 0.3 M $(TBA)PF_6$ at a platinum electrode [scan rate 4 mV/s]. (b) Time-resolved electronic absorption spectra taken during reduction of (TPP)In(CH_3) in PhCN (0.3 M $(TBA)PF_6$). (c) Time-resolved electronic absorption spectra taken during oxidation of (TPP)In(CH_3) in PhCN (0.3 M $(TBA)PF_6$). The initial species in (b) and (c) are represented by a solid line.

Thin-layer voltammograms for the reductions are reversible, indicating the lack of indium-carbon bond cleavage after the addition of either one or two electrons. This is illustrated by the well-defined thin-layer voltammogram in Figure 4a and the reversible thin-layer electronic absorption spectra shown in Figure 4b. Similar spectra were obtained for each of the singly reduced $[(TPP)In(R)]^-$ species, and maximum absorbance wavelengths are listed in Table V. These spectra are characteristic of anion

Table V. Maximum Absorbance Wavelengths (λ_{max}, nm) and Corresponding Molar Absorptivities ($\epsilon \times 10^{-3}$) for the Reduced $[(OEP)In(R)]^-$ and $[(TPP)In(R)]^-$ in PhCN (0.3 M$(TBA)PF_6$)

porphyrin	R	λ, nm ($\epsilon \times 10^{-3}$)				
OEP	$CH(CH_3)_2$	369 (79)	456 (80)	643 (24)	701 (23)	844 (21)
	C_4H_9	361 (46)	452 (86)	650 (17)	702 (15)	843 (14)
	C_2H_5	381 (29)	455 (45)		712 (24)	839 (34)
	CH_3	359 (87)	445 (139)	648 (50)	682 (48)	838 (48)
	C_6H_5		430 (161)		702 (25)	815 (36)
	$C_2H_2C_6H_5$		447 (155)	648 (76)	689 (74)	839 (20)
	$C_2C_6H_5$		435 (266)	646 (81)		831 (110)
TPP	$C(CH_3)_3$	390 (84)	481 (91)		799 (45)	898 (42)
	$CH(CH_3)_2$	383 (110)	475 (178)	721 (52)	787 (54)	899 (50)
	C_4H_9	353 (141)	471 (311)		778 (61)	896 (60)
	C_2H_5	373 (61)	474 (109)		782 (50)	895 (41)
	CH_3	349 (84)	471 (202)		774 (61)	899 (45)
	C_6H_5	374 (127)	468 (250)		770 (71)	897 (49)
	$C_2H_2C_6H_5$	357 (81)	438 (201)		796 (30)	875 (35)
	$C_2C_6H_5$	352 (41)	453 (263)		741 (44)	879 (30)

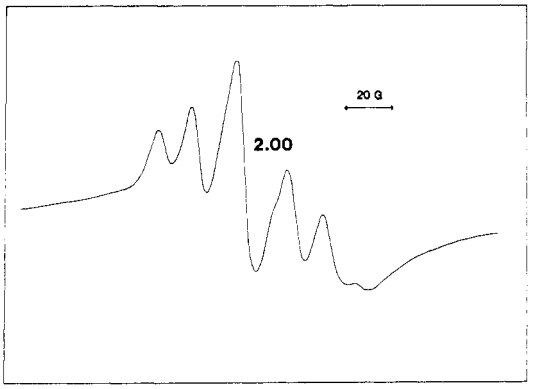

Figure 5. ESR spectrum of (TPP)In(CH_3) recorded at 115 K after reduction at −1.45 V in pyridine (0.1 M (TBA)PF_6).

radicals[46] and closely resemble, but are not identical with, spectra of singly reduced (TPP)InCl or (TPP)InClO_4 in the same media.[35] Specifically, for the case of [(TPP)In(CH_3)]$^-$ (Figure 4b), a peak is present at 353 nm that is not present for reduced (TPP)InClO_4 or (TPP)InCl. This strongly suggests that the CH_3 group remains bound after reduction and is also consistent with the reversibility of the thin-layer voltammograms.

Electrochemical Measurements in Pyridine (0.1 M (TBA)PF_6). The cyclic voltammogram of (TPP)In(CH_3) recorded in neat pyridine shows two reversible reduction waves at −1.08 and −1.52 V, but no oxidation waves are recorded in the solvent potential range. The first reduction is anodically shifted by 0.16 V from the value recorded in CH_2Cl_2. This difference may be due to changes in solvation (complexation) as well as different liquid-junction potentials of the two solvents. Under our experimental conditions, an anodic difference of 0.04 V is observed between the oxidation of ferrocene in neat pyridine and in CH_2Cl_2. Thus, after correction for liquid-junction potential effects, there remains a 0.12 V shift that is indicative of coordination of the reduced complex by the solvent, leading to a six-coordinate [(TPP)In(CH_3)(py)]$^-$ species. This binding of reduced indium–alkyl porphyrins by pyridine is in accordance with the mechanism suggested for the insertion of CO_2 into the indium–carbon bond.[34] Irradiation of a solution containing (TPP)In(CH_3) in benzene/pyridine leads to a species whose ESR spectrum suggests reduction of the neutral In(III) complex. In this present study, the same ESR spectrum was recorded after the one-electron reduction of (TPP)In(CH_3) in neat pyridine. Its trace is represented in Figure 5. The signal centered at $g = 2.00$ suggests a radical anion, but the large peak width (150 G) and the superhyperfine structure indicate a significant interaction between the anion radical and the central metal ion. The one-electron reduction of the other (TPP)In(R) complexes gives the same ESR spectrum in pyridine, thus also suggesting an interaction between the indium metal and the π orbitals of the ring system.

Oxidations of (TPP)In(R) and (OEP)In(R) in CH_2Cl_2 (0.1 M (TBA)PF_6). Six of the seven complexes in the (TPP)In(R) series undergo three single-electron oxidations, of which only the last two are reversible. A seventh σ-bonded complex, (TPP)In(C_6H_5), differs from the remaining series in that a reversible oxidation can be obtained for the first electron abstraction. A similar result was observed for the (OEP)In(R) series. Six of the seven complexes undergo an initial irreversible oxidation while, for (OEP)In(C_6H_5), an initial reversible oxidation can be obtained at low temperature.

A cyclic voltammogram of (TPP)In(C_6H_5) is shown at room temperature and at −10 °C in Figure 6. At room temperature (Figure 6a), the first couple (at $E_{pa} = 0.97$ V) is only partially reversible at a scan rate of 100 mV/s and three additional waves are observed (at $E_{1/2} = 1.20$, 1.45, and 1.53 V). As will be shown below, two of the waves (at 1.20 and 1.53 V) correspond to the

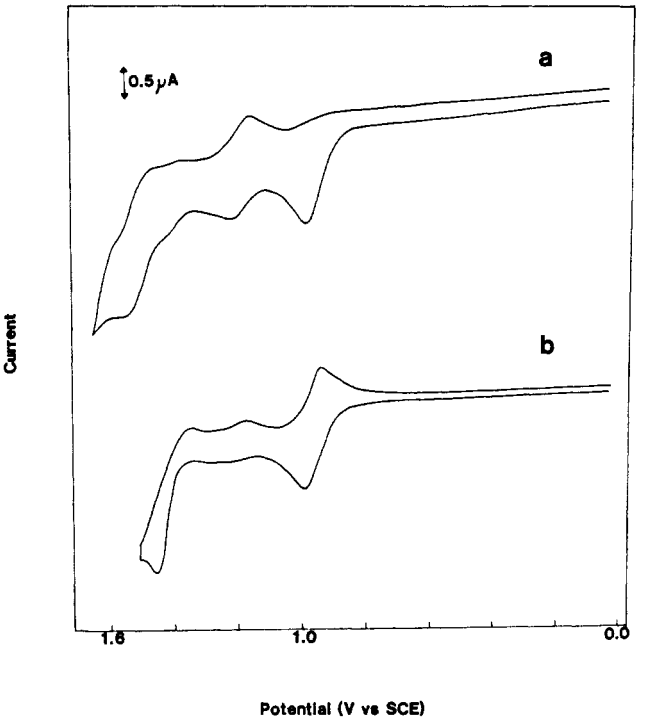

Figure 6. Cyclic voltammograms of (TPP)In(C_6H_5) in CH_2Cl_2 (0.1 M (TBA)PF_6). Voltammograms were recorded at (a) +20 °C and (b) −10 °C.

oxidation of [(TPP)In]$^+$, which is generated as a decomposition product after the initial one-electron abstraction.

Lowering the temperature to −10 °C resulted in a substantial increase in the reversibility of the first oxidation as well as a decrease in the current associated with the oxidations at 1.20 and 1.50 V. This is shown in Figure 6b. Values of $E_{pa} - E_{pc}$ were 55 ± 5 mV for the first oxidation at −10 °C, and $i_{pa}/i_{pc} = 1.0$. Both of these results suggest that the initial reversible abstraction of one electron occurs as shown by eq 4. The half-wave potential

$$\text{(TPP)In}(C_6H_5) \rightleftarrows [\text{(TPP)In}(C_6H_5)]^{+\cdot} + e^- \qquad (4)$$

for the above reversible oxidation is 0.94 V in CH_2Cl_2 (0.1 M-(TBA)PF_6). This compares with an $E_{1/2}$ value of 1.20 V for the oxidation of (TPP)InClO_4 in the same solvent/supporting electrolyte mixture. The direction of the potential shift on going from (TPP)InClO_4 to (TPP)In(C_6H_5) is similar to that between (TPP)FeClO_4 ($E_{1/2} = 1.10$ V) and (TPP)Fe(C_6H_5) ($E_{1/2} = 0.61$ V),[45] but the total magnitude of the shift as a function of bound ligand is smaller in the case of the indium series. For the case of (TPP)Fe(C_6H_5), the initial oxidation has been suggested to take place at the orbitals of the iron atom (generating Fe(IV)), and the first oxidation potential of the C_6H_5–iron(III) complex is shifted by 0.49 V with respect to the ClO_4^- derivative.[45] In the case of (TPP)InClO_4 and (TPP)In(C_6H_5) the difference in potential is only 0.26 V, possibly due to the fact that both complexes are reduced at the π-ring system. However, the singly oxidized (P)In(R) species is highly reactive (as is the oxidized (P)Fe(R)),[45] which argues against the π-ring system as the site of the initial electron abstraction in the case of indium.

Attempts were made to stabilize the product of the first oxidation, but at all temperatures only the spectra of [(TPP)In]$^+$ could be obtained after bulk electrolysis. This suggests a cleavage of the indium–carbon bond as shown by eq 5. The phenyl radical

$$[\text{(TPP)In}(C_6H_5)]^{+\cdot} \rightleftarrows [\text{(TPP)In}]^+ + [C_6H_5]\cdot \qquad (5)$$

generated after cleavage of the indium–carbon bond was not monitored, but this species is highly reactive and it is expected that rapid coupling to form biphenyl would occur on the cyclic voltammetric time scale. The formation of [TPPIn]$^+$ as shown in eq 5 should result in two additional waves (at $E_{1/2} \approx 1.20$ and ~1.50 V), and this is what is observed in Figure 6b.

(46) Fajer, J.; Borg, D. C.; Forman, A.; Felton, R. H.; Vegh, L.; Dolphin, D. Ann. N.Y. Acad. Sci. **1973**, *206*, 349.

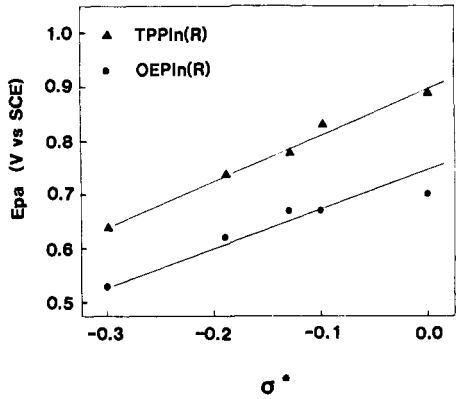

Figure 7. Plot of E_{pa} vs. σ^* for (TPP)In(R) and (OEP)In(R) where R stands for one of the σ-bound ligands listed in Tables III and IV.

Peak potentials for all of the σ-bonded compounds in CH_2Cl_2 (0.1 M $(TBA)PF_6$) are summarized in Tables III and IV. The first oxidation process is well-defined for all of the complexes, and diffusion-controlled, one-electron-transfer shapes of $E_p - E_{p/2} = 0.060 \pm 0.010$ V are obtained. With the exception of $(P)In(C_6H_5)$, no reverse reduction peak was present for the first oxidation at any scan rate in CH_2Cl_2, thus suggesting the presence of a rapid and irreversible chemical reaction following electron transfer, i.e., an EC mechanism as shown in eq 5. This mechanism is also suggested by the predicted 0.03 V anodic shift of peak potential with 10-fold increase in scan rate, as well as by the constant peak current increase with the square root of scan rate.

The peak potential for the first oxidation varied between 0.64 and 0.92 V for the (TPP)In(R) series in CH_2Cl_2 and between 0.62 and 0.81 V for the (OEP)In(R) series in the same solvent. Values of the substituent constant for the R group are given in Tables III and IV, and for five of the six complexes in the (TPP)In(R) series, a linear relationship is observed. This plot is shown in Figure 7 and yields slopes of $\Delta E_p/\Delta\sigma^*$ approximately 10 times larger than those for reduction of the same compound. This 10-fold increase in substituent effect can be explained on the basis of large interactions between the site of oxidation and the electron-donating or electron-withdrawing R groups[42] and suggests an initial abstraction either from In(III) or from an orbital of the alkyl group that is closely overlapped with an orbital of the metal. In any case, the singly oxidized species is not stable, and rapid cleavage of the indium–carbon bond occurs.

According to electrochemical theory the rate of an irreversible chemical reaction following electron transfer may be calculated by the shift of E_p from the reversible value of $E_{1/2}$ in the absence of the chemical reaction.[47] For electrooxidations, the peak potential shift would be in a negative direction so that for the specific case of the compounds in this study one can say that the relative rate of cleavage follows the R group electron donicity which is as follows:[42] $C(CH_3)_3 > CH(CH_3)_2 > C_4H_9 > C_2H_5 > CH_3 > C_2H_2C_6H_5 > C_6H_5$. This order is based on the increasing negative shift of potential for the first oxidation. For a given constant value of $E_{1/2}$, the more negative the peak potential, the larger the rate constant for cleavage of the metal–carbon bond (as shown in eq 5 for $[(TPP)In(C_6H_5)]^{+\cdot}$). The most stable predicted In(III) compound is that which contains the σ-bonded phenyl group, and this is confirmed by the experimental data. Unfortunately, the reversible $E_{1/2}$ values could not be obtained for any of the complexes except $(P)In(C_6H_5)$, and for this reason, valid calculations of actual rate constants are not possible.

A partial reduction peak for electrogenerated $[(TPP)In(C_6H_5)]^+$ is evident at room temperature (see Figure 6), and from values of i_{pa}/i_{pc} at a given scan rate, the rate of metal–carbon cleavage according to eq 5 can be easily calculated. Data for the cleavage of $[C_6H_5]\cdot$ from $[(TPP)In(C_6H_5)]^+$ was analyzed according to the ratio of peak currents[47] and gave a self-consistent first-order rate constant of 1.2 s^{-1} at 20 °C and 0.25 s^{-1} at −10 °C. Similar types of calculations were not possible for the remaining $[(P)In(R)]^+$ complexes that have no reversible rereduction peak.

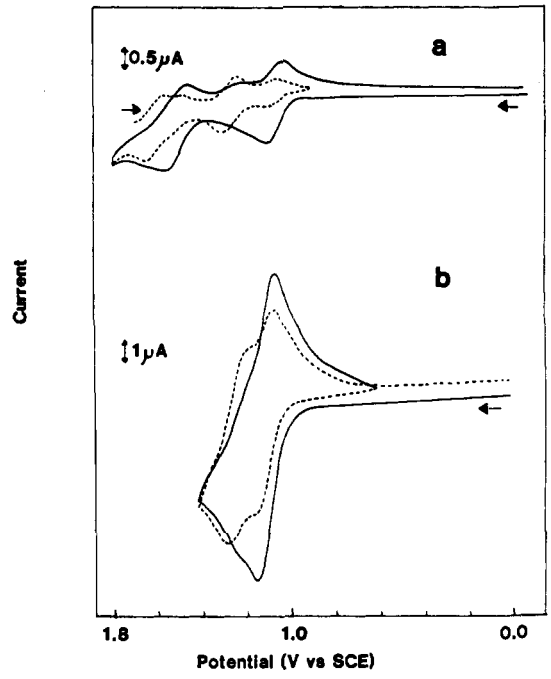

Figure 8. (a) Cyclic voltammogram of $(TPP)In(C_2C_6H_5)$ in PhCN (0.1 M $(TBA)PF_6$) at a platinum electrode [scan rate 100 mV/s]: initial potential 0.0 V (—); initial potential 1.6 V (---). (b) Cyclic voltammogram of the same solution at a thin-layer platinum electrode [scan rate 4 mV/s].

It may be significant to note that the $(TPP)In(C_6H_5)$ derivative does not fit the plot of E_p vs. σ^*. In a like manner, the peak potential for oxidation of $(OEP)In(C_6H_5)$ also does not fit a linear free energy plot for the (OEP)In(R) series. This could suggest a mechanism that is different for the R = C_6H_5 complexes than for the other σ-bonded complexes. However, as will be shown in later sections, there is no deviation in plots of E_{pa} vs. the ratio of molar absorptivities taken from the electronic absorption spectra for each (P)In(R) of the respective complexes.

The second and third oxidations of (TPP)In(R) and (OEP)In(R) are independent of the substituent constant, and the half-wave potentials for all complexes in a given series are invariant, regardless of the alkyl group bonded to the metal. In addition, the values of $E_{1/2}$ for these two processes are at potentials identical with those observed for the reversible oxidation of the respective $(TPP)InClO_4$ ($E_{1/2}$ = 1.20 and 1.51 V) or $(OEP)InClO_4$ species ($E_{1/2}$ = 1.12 and 1.40 V) in CH_2Cl_2 (0.1 M $(TBA)PF_6$). This fact also suggests cleavage of the indium–carbon bond after the first oxidation of these compounds. Finally, the conclusion of an indium–carbon bond cleavage is strengthened by bulk electrolysis experiments performed on both $(TPP)In(CH_3)$ and $(TPP)In(C(CH_3)_3)$ in CH_2Cl_2 (0.1 M $(TBA)PF_6$). Bulk electrolysis at 1.0 V leads to solutions of the same brown color for both compounds after the removal of one electron. A cyclic voltammogram of the brown solution shows reversible oxidation waves at 1.18 and 1.50 V and reversible reduction waves at −1.07 and −1.46 V. The resulting UV–visible spectrum after the initial oxidation is not of a "hyper" type but rather has a Soret band at 421 and Q bands at 558 and 597 nm, respectively. All of these data as well as the lack of an ESR signal for the singly oxidized species firmly suggest the formation of $(TPP)In^+PF_6^-$ as shown by eq 5.

Electrode Reactions of $(TPP)In(C_2C_6H_5)$ and $(OEP)In(C_2C_6H_5)$ in PhCN (0.1 M $(TBA)PF_6$). Both $(TPP)In(C_2C_6H_5)$ and $(OEP)In(C_2C_6H_5)$ are unstable in $CHCl_3$ and CH_2Cl_2, and a cleavage of the indium–carbon bond readily occurs in these solvents. In contrast, excellent stability is obtained in PhCN. For

(47) Nicholson, R. S.; Shain, I. *Anal. Chem.* **1964**, *36*, 707.
(48) Cole, S. J.; Curthoys, G. C.; Magnusson, E. A.; Phillips, N. J. *Inorg. Chem.* **1972**, *11*, 1024.

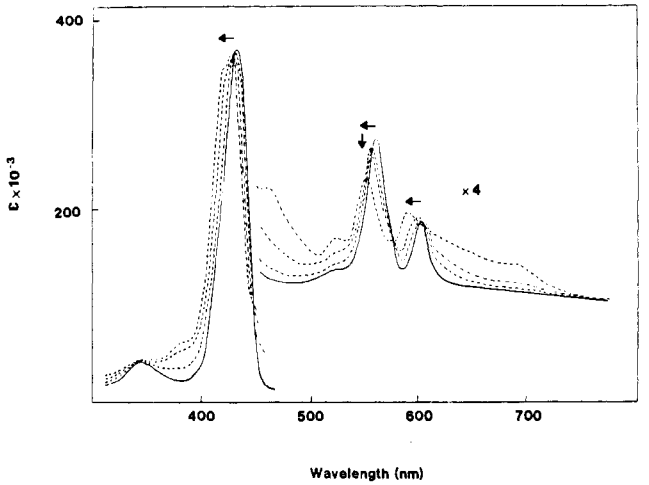

Figure 9. Time-resolved electronic absorption spectra taken during oxidation of (TPP)In($C_2C_6H_5$) at 1.22 V in PhCN (0.3 M (TBA)PF_6): (1) after 10 s; (2) after 30 s; (3) after 50 s; (4) after 60 s.

Table VI. Half-Wave Potentials (V vs. SCE) for the Oxidation and Reduction of (P)In($C_2C_6H_5$) and (P)InClO_4 in PhCN in 0.1 M (TBA)PF_6

	oxidation		reduction	
complex	1st	2nd	1st	2nd
(TPP)In($C_2C_6H_5$)[a]	1.15	1.60[b]	−1.06	−1.51
(TPP)InClO_4	1.26	1.59	−1.02	−1.46
(OEP)In($C_2C_6H_5$)	1.01	1.44	−1.31	...
(OEP)InClO_4	1.04	1.28	−1.30	−1.78

[a] Additional oxidation peaks are also present due to the reaction of generated (P)InPF_6 (see text). [b] Only small currents are observed for this process due to the rapid decomposition of singly oxidized [(P)In($C_2C_6H_5$)]$^{+\cdot}$.

this reason, all electrochemical and spectroscopic measurements of these compounds were carried out in this solvent.

A typical cyclic voltammogram of (TPP)In($C_2C_6H_5$) in PhCN (0.1 M (TBA)PF_6) is shown in Figure 8. Unlike the other (TPP)In(R) complexes, two reversible reductions and two reversible oxidations are obtained at room temperature. The reductions occur at −1.04 and −1.49 V while the oxidations occur at 1.15 and 1.58 V. These values are listed in Table VI which also includes potentials for oxidation/reduction of (OEP)In($C_2C_6H_5$) and the corresponding (TPP)InClO_4 and (OEP)InClO_4 derivatives in PhCN.

As seen in Table VI the reversible potentials for oxidation and reduction of (P)In($C_2C_6H_5$) are much closer to those of the ionic In(III) species than to potentials of the other σ-bonded In(III) species investigated in this study (see Tables III and IV). This is true despite spectroscopic data that clearly indicate a σ-bonded carbon ligand. Of most surprise is that the neutral (P)In($C_2C_6H_5$) complexes are the least stable species in solution (and rapidly undergo decomposition) yet they are the most stable of the σ-bonded species after oxidation by one electron to yield [(P)In(R)]$^+$. A relatively good stability is also obtained after the abstraction of the second electron from (P)In($C_2C_6H_5$), and at room temperature, substantial quantities of the doubly oxidized [(P)In($C_2C_6H_5$)]$^{2+}$ can be generated at the electrode surface. These two oxidation reactions are represented by eq 6 and 7 and are

$$(P)In(C_2C_6H_5) \rightleftarrows [PIn(C_2C_6H_5)]^{+\cdot} + e^- \quad (6)$$

$$[(P)In(C_2C_6H_5)]^{+\cdot} \rightleftarrows [(P)In(C_2C_6H_5)]^{2+} + e^- \quad (7)$$

illustrated by the cyclic voltammograms of (TPP)In($C_2C_6H_5$) in Figure 8. On the same figure, a thin-layer cyclic voltammogram is represented that illustrates the cleavage of the indium–carbon bond on the longer time scale of these experimental conditions (~2 min).

On initial cyclic voltammetric scans, oxidation peaks of (TPP)In($C_2C_6H_5$) are found at $E_{1/2}$ = 1.15 and 1.60 V. However, upon multiple scans, new peaks appear at 1.35 and 1.69 V. The initially observed peaks at 1.15 and 1.60 V correspond to the reversible half-wave potentials for the initial oxidation of (TPP)In($C_2C_6H_5$). In contrast, the waves formed upon repeated scans

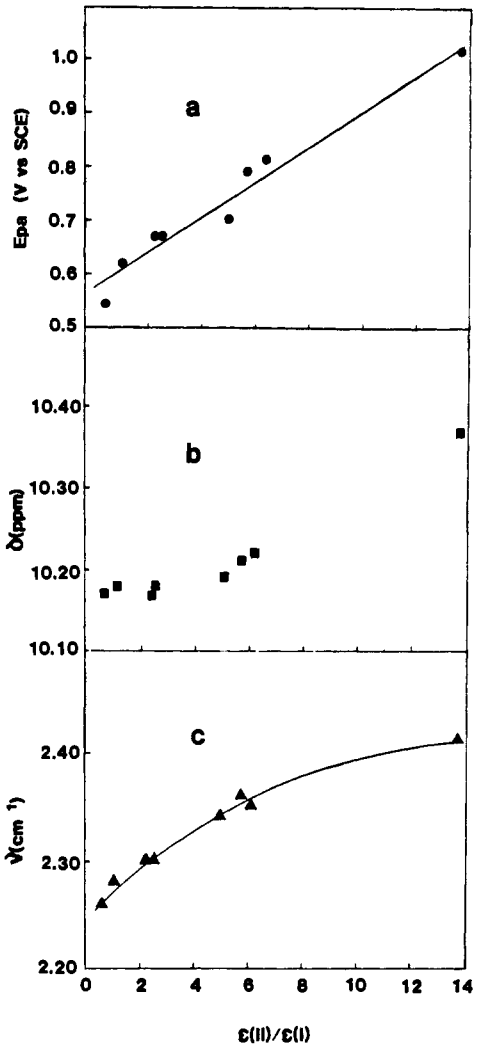

Figure 10. Plot showing the dependence of the first oxidation potential (E_{pa}), the NMR shifts (δ), and the spectral wavelengths for band II (cm^{-1}) of (OEP)In(R) complexes on the ε(II)/ε(I) ratio.

Table VII. Summary of (OEP)In(R) Physicochemical Properties Used in Free Energy Correlations

complex	R	ε(II)/ε(I)[a]	E_{pa},[b] V vs. SCE	δ	ν,[c] $cm^{-1} \times 10^{-6}$
1	$C(CH_3)_3$	0.64	0.53	10.17	2.26
2	$CH(CH_3)_2$	1.09	0.62	10.18	2.28
3	C_4H_9	2.39	0.67	10.17	2.30
4	C_2H_5	2.48	0.67	10.18	2.30
5	CH_3	5.04	0.70	10.19	2.34
6	C_6H_5	5.85	0.79	10.21	2.36
7	$C_2H_2C_6H_5$	6.18	0.81	10.22	2.35
8	$C_2C_6H_5$	13.88	1.01	10.37	2.41

[a] Data taken from Table II. [b] Data taken from Table IV. [c] Data for band I taken from Table II.

are due to the oxidation of $(TPP)InPF_6$ which is generated as a product of a chemical reaction at the electrode surface. This conclusion agrees with data for all of the (TPP)In(R) complexes, each of which has reversible second and third oxidation potentials at 1.35 and 1.69 V in PhCN.

More direct proof for conversion of $(TPP)In(C_2C_6H_5)$ to $(TPP)InPF_6$ comes from spectral monitoring of the electrooxidation products and from the analysis of cyclic voltammograms that were scanned in a negative direction after holding the potential at 1.8 V for 30 s. An example of one such voltammogram is shown by the dotted lines in Figure 8a. After the potential is held at 1.8 V, four sets of oxidation–reduction peaks are observed. The peaks at 1.35 and 1.69 V are due to reactions of $(TPP)InPF_6$ and are identical with peaks present in cyclic voltammograms of $(TPP)InClO_4$ in PhCN (0.1 M $(TBA)PF_6$) that are initiated after a similar oxidation at this potential for 30 s. In these conditions a ligand exchange occurs in solution that is as represented by eq 8 and 9.

$$[(TPP)In(C_2C_6H_5)]^{2+} + PF_6^- \rightarrow [(TPP)In(PF_6)]^{2+} + [(C_2C_6H_5)]^- \quad (8)$$

$$[(TPP)InClO_4]^{2+} + PF_6^- \rightleftarrows [(TPP)In(PF_6)]^{2+} + ClO_4^- \quad (9)$$

Conversion of $(TPP)In(C_2C_6H_5)$ to $(TPP)InPF_6$ is also seen on the thin-layer cyclic voltammetric time scale as illustrated in Figure 8b. Initial scans from 0.0 to 1.4 V show a major oxidation–reduction peak at 1.15 V and a very small set of peaks at 1.35 V. However, when the scan is reversed at 0.8 V and a second positive potential sweep carried out, the ratio of the currents change such that the peak at 1.35 V has become the major oxidation peak while the one at 1.15 V has significantly decreased in magnitude. This is illustrated by the dotted lines in Figure 8b.

Time-resolved spectra recorded at 1.22 V first indicate the formation of a radical-like species with isosbestic points observed during the first few seconds. This is illustrated in Figure 9. At longer times the isosbestic points disappear and a new series of spectra are recorded that resemble the (TPP)InCl absorption spectrum. These spectra are probably due to $(TPP)InPF_6$. Unfortunately, this is the only condition where spectral identification of the oxidized species has been possible.

Correlations Between Electrochemical and Spectroscopic Data. Numerous correlations are possible between electrochemical and spectroscopic properties of the σ-bonded (P)In(R) complexes in this study. This is best illustrated by the (OEP)In(R) series where ^1H NMR, electrochemistry, and electronic absorption spectroscopy data are all available under similar solution conditions. The relevant data from each of these measurements are given in Table VII, and a summary of three correlations is given in Figure 10. As seen in this figure, plots of E_{pa} (in V), δ (in ppm), and ν of band I (in cm^{-1}) are either linear or curvilinear with the ratio $\epsilon(II)/\epsilon(I)$.

For the investigated series of compounds, the molar absorptivity ratio directly relates to the electron donicity properties of the R group and provides a good measure of the electron density on the porphyrin π system as well as on the central metal. The higher the σ-bonded character of the indium–carbon bond, the lower the ratio of $\epsilon(II)/\epsilon(I)$. An evolution from pure σ-bonded character of the indium–carbon bond for the $(P)In(C(CH_3)_3)$ complexes to an ionic-like character for the indium–carbon bond of the $(P)In(C_2C_6H_5)$ complexes occurs, and this is reflected by the UV–visible spectra, the NMR spectra, and the electrochemical data. However, the electrooxidation properties of the complexes appear to be the most sensitive to this effect, and a shift of about 400 mV is observed between the oxidation potential of the complex containing the strongest σ-bonding and the weakest σ-bonding R group. It is especially interesting to note that the complexes that show the most σ-bonding character of the R group are also the most unstable toward oxidation. Also, $(P)In(C_6H_5)$ derivatives appear to be the only species with a σ bond that is stable in the oxidized form.

Acknowledgment. The support of the National Science Foundation (Grant 8215507) is gratefully acknowledged.

Registry No. **1**, 63036-71-5; **2**, 72340-07-9; **2**$^-$, 96394-14-8; **3**, 63036-70-4; **3**$^-$, 96363-82-5; **4**, 63036-69-1; **4**$^-$, 96363-83-6; **5**, 63288-51-7; **5**$^-$, 96363-84-7; **6**, 63074-32-8; **6**$^-$, 96363-85-8; **7**, 72340-08-0; **7**$^-$, 96363-86-9; **8**, 72340-09-1; **8**$^-$, 96363-87-0; $(TPP)In(C(CH_3)_3)$, 63036-67-9; $[(TPP)In(C(CH_3)_3)]^-$, 96363-88-1; $(TPP)In(CH(CH_3)_2)$, 72340-10-4; $[(TPP)In(CH(CH_3)_2)]^-$, 96363-89-2; $(TPP)In(C_4H_9)$, 63036-66-8; $[(TPP)In(C_4H_9)]^-$, 96363-90-5; $(TPP)In(C_2H_5)$, 63036-65-7; $[(TPP)In(C_2H_2)]^-$, 96363-91-6; $(TPP)In(CH_3)$, 63074-31-7; $[(TPP)In(CH_3)]^-$, 96363-92-7; $(TPP)In(C_6H_5)$, 63036-68-0; $[(TPP)In(C_6H_5)]^-$, 96394-15-9; $(TPP)In(C_2H_2C_6H_5)$, 72340-11-5; $[(TPP)In(C_2H_2C_6H_5)]^-$, 96363-93-8; $[(TPP)In(C_2C_6H_5)]^-$, 96363-94-9; $(TPP)InClO_4$, 91312-86-6; $(OEP)InClO_4$, 96363-81-4; $(TBA)PF_6$, 3109-63-5; In, 7440-74-6.